NUMERICAL STUDY OF THE UPSTREAM WAVE EXCITATION MECHANISM:

1. NONLINEAR PHASE BUNCHING OF BEAM IONS

Masahiro HOSHINO and Toshio TERASAWA

Institute of Space and Astronautical Science,
6–1, Komaba 4-chome, Meguro-ku, Tokyo 153

Abstract: By means of the particle simulation, we study the excitation mechanism of low frequency (0.01–0.05 Hz) upstream hydromagnetic waves. Initially, we observe excitation of the right-hand polarized waves propagating parallel to the field-aligned ion beam, which is given as the free energy source. In the nonlinear stage, we observed the phase space bunching of beam ions by the excited waves. We apply this bunching effect to the explanation of 'gyrophased bunched' ions observed in the foreshock region.

1. Introduction

ASBRIDGE *et al.* (1968), FAIRFIELD (1969), and SCARF *et al.* (1970) made pioneering studies on the backstreaming ions and associated large amplitude magnetic fluctuations observed in the upstream region of the earth's bow shock. ISEE observations show that there are three distinct types of ion populations, namely 'reflected', 'intermediate', and 'diffuse' ions (GOSLING *et al.*, 1978; PASCHMANN *et al.*, 1979, 1981; BONIFAZI *et al.*, 1980; BONIFAZI and MORENO, 1981a, b; GREENSTADT *et al.*, 1980). Large amplitude low frequency (0.01–0.05 Hz) hydromagnetic waves are observed with the diffuse ions, which are characterized by a broad angular distribution (HOPPE *et al.*, 1981, 1982). 'Intermediate' ions, which are characterized by a crescent-shaped distribution in the velocity space, are also observed with large amplitude low frequency waves in the foreshock region. On the other hand, in conjunction with the 'reflected' ions, which have a beam-like distribution, only higher-frequency waves (~ 1 Hz) with a weak amplitude are observed. (Note that these high frequency waves are now considered to be excited by the backstreaming electrons (SENTMAN *et al.*, 1983)). In this paper, we shall concentrate on the study of the excitation mechanism of the low frequency waves.

For the origin of these low frequency hydromagnetic waves, FAIRFIELD (1969), BARNES (1970), GARY *et al.* (1981) and SENTMAN *et al.* (1981) proposed an ion beam instability process, in which backstreaming ions, presumably the 'reflected' ions, excite the right-hand polarized hydromagnetic waves through the cyclotron resonance interaction,

$$\omega - k_{\|} V_{\mathrm{b}} = -\Omega_{\mathrm{i}} , \qquad (1)$$

where ω is the angular frequency in the solar wind rest frame, $k_{\|}$ the parallel wave

number, V_b the magnitude of beam velocity, and Ω_i the ion (proton) cyclotron frequency. The maximum growth rate ($\sim 0.1 \, \Omega_i$) is expected for the waves propagating along the ambient magnetic field in the same direction as the beam ions. Recent results by HOPPE and RUSSELL (1983) and WATANABE and TERASAWA (1984) confirmed that the observed low frequency waves have characteristics consistent with the above theoretical analysis. Since the phase velocity of these waves is close to the Alfvén velocity V_a, these waves in the spacecraft frame are observed to be polarized in the left hand (anomalous Doppler effect caused by the super Alfvénic solar wind flow).

Recently, WINSKE and LEROY (1984) have studied the evolution of the electromagnetic ion beam instability stated above by means of the numerical simulation. In the linear stage of the instability their results confirm the theoretical expectation. In the nonlinear stage, they observed pitch angle scattering effect, which they consider to be the process of the 'diffuse' ion production out of the 'reflected' ions. They further observed a decay instability of the excited waves.

However, the above ion species, namely 'reflected', 'intermediate', and 'diffuse' ions, may not complete the list of the upstream particle populations. GURGIOLO et al. (1981) and EASTMAN et al. (1981) presented evidence for another population of upstream ions that they termed 'gyrophase bunched'. These 'gyrophase bunched' ions are characterized by their non-gyrotropic behavior. GURGIOLO et al. (1983) proposed a mechanism to create gyrophase bunched distribution of ions: They assume the injection of gyrophase bunched ions at the bow shock. Due to the finite width in the velocity distribution, these ions are then subjected to the gyrophase mixing. These authors followed the successive evolution of the phase space distribution, and applied their result to the explanation of the 'diffuse' ion formation from the 'reflected' ions.

GOSLING et al. (1982) observed an injection of gyrophase bunched ions which would be produced by the specular reflection process at the quasi-parallel bow shock. After the injection, the gyrophase mixing is expected to occur quite rapidly, so that these ions are gyrophase bunched within a few gyroradii from the bow shock (GURGIOLO et al., 1983). GURGIOLO et al. (1981) and EASTMAN et al. (1981), on the other hand, noted that the gyrophase bunched ions are observed throughout the foreshock region. It seems, therefore, difficult to explain these observations by GURGIOLO et al.'s mechanism alone.

GREENSTADT et al. (1982) suggested a possible connection between gyrophase bunched ions and observed large amplitude magnetic variations associated with the quasi-parallel bow shock. THOMSEN et al. (1985) showed an example of the simultaneous observations of the large amplitude hydromagnetic waves and the 'gyrophase bunched' ions. From the numerical study of nonlinear behavior of these waves excited by the ion beam cyclotron instability process, we propose in this paper a new mechanism to produce these 'gyrophase bunched' ions: In the nonlinear stage of this instability, beam ions are bunched in the phase space by the excited waves. We suggest that this 'wave-phase' bunching process is the origin of 'gyrophase bunched ions'.

2. Simulation Model

Our simulations were performed with a one-dimensional electromagnetic implicit particle code in which both ions and electrons are treated as discrete particles (HOSHINO and TERASAWA, in preparation). In our simulation model we only treat waves whose propagation directions are parallel and anti-parallel to the ambient magnetic field (the x direction). The system is assumed to be periodic in the x direction. Figure 1 shows a schematic illustration of our simulation system. Initially we put beam ions as a free energy source. We then follow the electromagnetic evolution of the system.
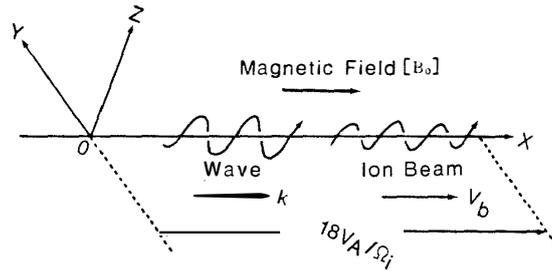

Fig. 1. Model of the present simulations with one-dimensional, electromagnetic implicit code.

From the linear stability analysis, electrons are not expected to play any important role in the ion beam instability process. This expectation, which is confirmed in our simulation, is a basis of the application of the hybrid simulation code (fluid electrons+particle ions) to the same instability process (WINSKE and LEROY, 1984). Using a full-particle description for both ions and electrons, we can be free from any *ad hoc* assumption. A drawback of the use of the full particle code, however, is a large demand for the computer resources. Because of this reason, our simulation is limited in the spatial size $(L_x = 18V_a/\Omega_i)$. As a result, we can only treat an instability process with a slow ion beam velocity ($\sim 2.5V_a$), since ions with a realistic beam velocity ($\geq 10V_a$) resonate with waves whose wavelength is longer than the feasible system size. Further, to save the CPU time, we use the higher beam density ($\sim 20\%$ of the background plasma) than the observed beam density ($\sim 1\%$). We could, however, treat in the simulation the same elementary physical process as in the fore-shock region (see the discussion section).

Initially the plasma density is set uniform, and the magnetic field has the x component (B_0) only. We assume that the plasma consists of three components, namely the background (medium) ions (denoted by the suffix 'm'), the beam ions ('b'), and the electrons ('e'), which have shifted Maxwellian distributions as given by,

$$f_m(V_{\parallel}, V_{\perp}) = C_N(n_0 - n_b) \exp\left[-m_i(V_{\parallel}^2 + V_{\perp}^2)/2T_m\right]$$

$$f_b(V_{\parallel}, V_{\perp}) = C_b n_b \exp\left[-m_i((V_{\parallel} - V_b)^2 + V_{\perp}^2)/2T_b\right] \tag{2}$$

$$f_e(V_{\parallel}, V_{\perp}) = C_N' n_e \exp\left[-m_e((V_{\parallel} - V_{ed})^2 + V_{\perp}^2)/2T_e\right],$$

where C_N, C_b and C_N' are normalization constants, V_b is a beam velocity. $V_{\parallel}$ and $V_{\perp}$ are the velocity components parallel and perpendicular to the ambient magnetic field. To make the system current-free, the electrons are moved with the velocity

$V_{ed} = V_b (n_b/n_0)$. We assume that the beam ion temperature (T_b) is equal to the background ion temperature (T_i), $T_b = T_m \equiv T_i$. The electron temperature T_e is set equal to 16 T_i. The plasma beta,

$$\beta \equiv \frac{8\pi n_0 (T_e + T_i)}{B_2^0} ,$$

is 0.4, mass ratio $m_i/m_e = 25$. The ion beam velocity V_b is taken to be 2.5 V_a. The beam density n_b is set to be 0.2 n_0. The ratio between the light velocity c and the Alfvén velocity V_a is taken to be 17.9, which is large enough to get a clear separation between the radiation branch $(\omega \sim kc)$ and the low frequency hydromagnetic branch $(\omega \sim kV_a)$.

Table 1. Simulation parameters in simulation unit.

Grid size	(ΔX)	1	Time step	(Δt)	0.05
Light velocity	(c)	10	Alfvén velocity	(V_a)	0.56
Ion thermal velocity	$(v_{th,i})$	0.0875	Electron thermal velocity	$(v_{th,e})$	1.75
Ion beam velocity	(V_b)	1.4	Electron drift velocity	(V_{ed})	0.28
Ion plasma frequency	(ω_{pi})	1.41	Electron plasma frequency	(ω_{pe})	7.07
Ion cyclotron frequency	(Ω_i)	0.08	Electron cyclotron frequency	(Ω_e)	2

The time step Δt is taken to be 0.1 Ω_e^{-1} (the reciprocal of the electron cyclotron frequency), in order to follow the electron gyromotion accurately. The grid size Δx is taken 0.141 V_a/Ω_i (or 0.175 times the electron Debye length). We use 128 spatial meshes and 4096 × 3 simulation particles for the beam ions, the background ions, and the electrons. (The mass and charge weights of the simulation particles for beam ions are 1/4 of the background ions.) These simulation parameters are tabulated in Table 1. As one of the checks of the simulation code, the total energy of the system is traced throughout the simulation runs. We found that the total energy was conserved within 2% error for the run described in the following.

3. Simulation Result

Figure 2 shows the energy histories of beam ions, background ions, electrons, and electromagnetic field. In the initial period $(0 < \Omega_i t < 16)$, the beam energy is slowly transferred to the background ion energy (in the motion parallel to the magnetic field). This energy transfer is caused by electrostatic ion acoustic waves excited in the system. Using the results by Lemons et al. (1979), Gary (1981) showed that the upstream ion beams $(V_b \gtrsim 10 \ V_a)$ are stable with respect to the ion acoustic waves excitation. From the linear stability analysis, however, our simulation system is found to be unstable to the excitation of this mode: There are the upper and lower thresholds of V_b for the ion acoustic waves to be unstable (Lemons et al., 1979), and the feasible choice of V_b for our simulations is within this unstable regime. Although these ion acoustic waves have a large growth rate $(\gamma \sim 1.6 \ \Omega_i)$, their saturation level is much lower than the electromagnetic waves excited later. We found that these electrostatic waves do not play a major role in the energy history. Note that the energy of electrons slightly increases during this 'ion acoustic phase', but remains almost constant after this phase
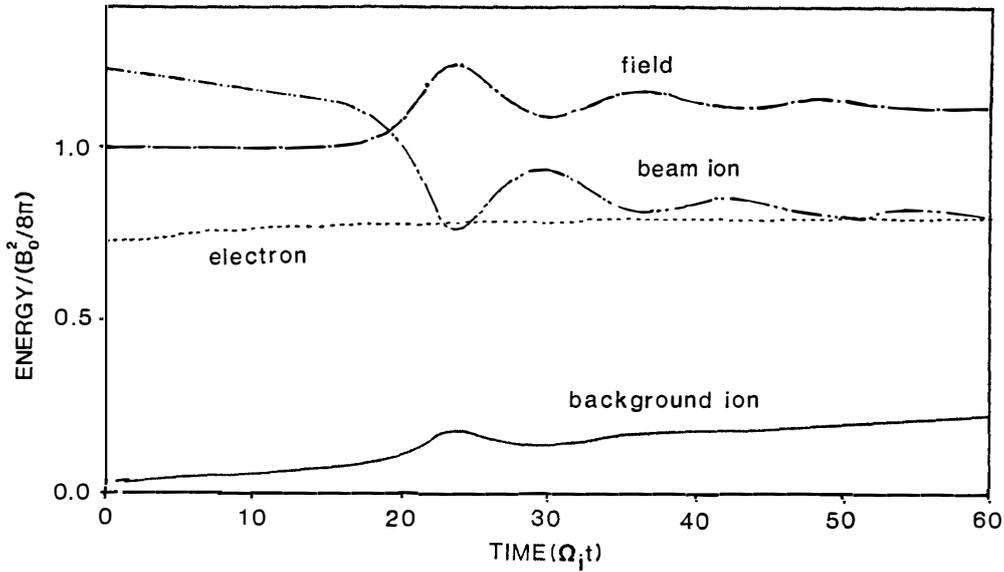
Fig. 2. *Energy histories for background ions, beam ions, electrons and the electromagnetic field.*
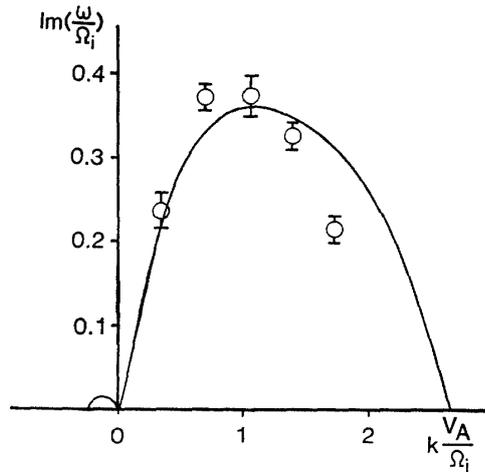

Fig. 3. *Linear growth rate ($\bar{\gamma}/\Omega_1$, solid curves) obtained from linear dispersion relation. Open circles with error bars are calculated from our simulation results.*

(Fig. 2).

During the next period ($16 < \Omega_i t < 24$) the ion beam energy is converted to the wave energies, which consist mainly of the magnetic field energy and the background ion energy (in the motion perpendicular to the ambient magnetic field). We confirm that excited waves have a right-hand polarization with respect to the ambient magnetic field. Open circles with bars in Fig. 3 show the observed growth rates for these waves of the modes $m = 1, 2, 3, 4,$ and 5, respectively. (The mode number m relates to the wavenumber k as $k = 2\pi m/L_x$). Solid curves in the figure show the theoretical growth rate (for $k > 0$ and $k < 0$) obtained from the dispersion relation for the right-hand polarized waves,

$$\omega^2 - k^2 c^2 + \frac{n_b}{n_0} \omega_{pi}^2 \frac{\omega - kV_b}{kV_{th,b}} Z\left(\frac{\omega - kV_b + \Omega_i}{kV_{th,b}}\right)$$

$$+\left(1-\frac{n_b}{n_0}\right)\omega_{pi}^2\ \frac{\omega}{kV_{th,m}}\ Z\left(\frac{\omega+\Omega_i}{kV_{th,m}}\right)$$ (3)

$$+\omega_{pe}^2\ \frac{\omega-kV_{ed}}{kV_{th,e}}\ Z\left(\frac{\omega-kV_{ed}-\Omega_e}{kV_{th,e}}\right)=0\ ,$$

where Z is the plasma dispersion function, ω_{pi} and ω_{pe} the ion and electron plasma frequency. $V_{th,j}$ (with $j=b, m$ and e) is the thermal velocity, $(2T_j/m_j)^{1/2}$, for each component. As seen in Fig. 3, the simulation results on the linear growth rates are in good agreement with the analytical results for the waves propagating parallel to the beam ($k>0$). The real frequency of the excited waves ($\sim 1.5\,\Omega_i$, for the waves of $m=3$, for example) is also consistent with the result of the linear theory ($1.8\,\Omega_i$). For the antiparallel direction ($k<0$), there is a weakly unstable branch (the nonresonant firehose branch). Since the expected wavelength for this firehose branch is longer than the system size and its growth rate is too small, this branch is not excited in our simulation.

After the time of $\Omega_i t=24$ (the 'nonlinear' phase, hereafter), we observed repeating exchange of the energy between the beam ions and the electromagnetic field. We interpret this oscillation to be caused by the phase bunching of beam ions in the wave fields. From the theory of phase bunching (Palmadesso and Schmidt, 1971; also see the discussion section), the oscillation period is expected to be

$$2\pi\left(\frac{m_i c}{eB_\perp kV_\perp}\right)^{1/2}\sim 15\,\Omega_i^{-1}\ ,$$

where we used the parameters suited for our simulation, $B_\perp/B_0=0.4$ (the wave amplitude in the nonlinear phase), $kV_a/\Omega_i=1.0$, and $V_\perp/V_a=0.45$. For $V_\perp$, we used the per-
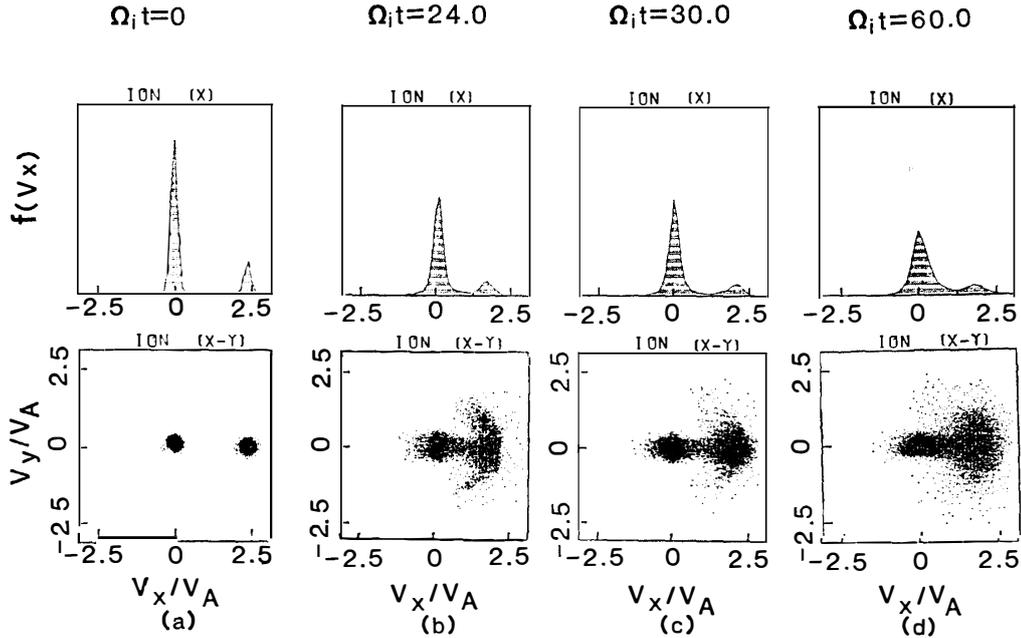

Fig. 4.   Simulation results: $f(V_x)-V_x$ (upper panel) and the phase space projection (V_x-V_y, lower panel) for both ion components at various times.

pendicular velocity acquired by the beam ions in the nonlinear phase.   This theoretical value is consistent with the observed oscillation period ($\sim 13\ \Omega_i^{-1}$).

The projected distribution function,

$$f(V_x) \equiv \int f(V_x,\ V_y,\ V_z;\ X)\mathrm{d}V_y\mathrm{d}V_z\mathrm{d}X\ ,$$

for the ion components (background+beam) is shown in the upper panels of Fig. 4, while their two-dimensional projection to the V_x-V_y plane is shown in the lower panels. Figure 4a represents the initial distributions ($\Omega_i t=0$). Figure 4b shows the distributions at $\Omega_i t=24$, when the wave growth ceases and the excited waves have the maximum amplitude ($\delta B/B_0 \sim 0.5$).   In the lower panel, we can see that the beam ions produce a crescent-shaped distribution, where the parallel beam energy is being released.   The effect of ion acoustic wave excitation is seen in Fig. 4b as widening of the thermal in the V_x for both the background and the beam ions.   During the nonlinear phase, the beam ions become more diffusive in the pitch angle distribution (Figs. 4c and 4d).   We also observe the heating of the background ions in the parallel direction in the nonlinear phase (Fig. 4d, the upper panel).
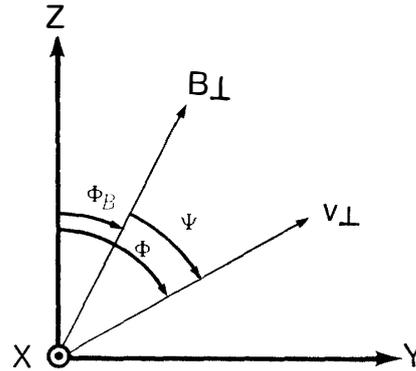

Fig. 5.   Definition of the phase angles for wave magnetic field (Φ_B), particles (Φ), and the difference between them ($\psi=\Phi-\Phi_B$).

To see the relation between the beam ions and the excited waves more closely, we plot in Fig. 6 the phase angle Φ for each particle, where Φ is defined as $\tan^{-1}\ (V_y/V_z)$ (see Fig. 5 for definition).   Three panels from the top of Figs. 6a to 6e show the phase space ($x-\Phi$) distributions for beam ions, electrons, and background ions, respectively.   The heavy dots in the same panels show the phase angles Φ_B of the waves defined as $\tan^{-1}\ (B_y/B_z)$.   The remaining two panels of Figs. 6a–6e show the spatial wave forms of B_y and B_z.   At the time of $\Omega_i t=9.6$ (Fig. 6a), transverse magnetic fields are in the noise level and the particles are distributed uniformly in this phase space. After the time of $\Omega_i t=18$ (Figs. 6b–6e), we see the excitation of more-or-less sinusoidal waves in the bottom two panels.   The phase angle of the waves increases toward the positive x direction, that is to say, these waves have left-hand polarization in space. Since they propagate toward the positive x direction, they have right-hand polarization in time.

The phase angle difference between the magnetic field and the background ions (the third panels from the top in Figs. 6b–6e) is around π, showing the property of the MHD waves (namely, the relation $\delta V=-\delta B/(4\pi n_0 m_i)^{1/2}$).   For the beam ions, on
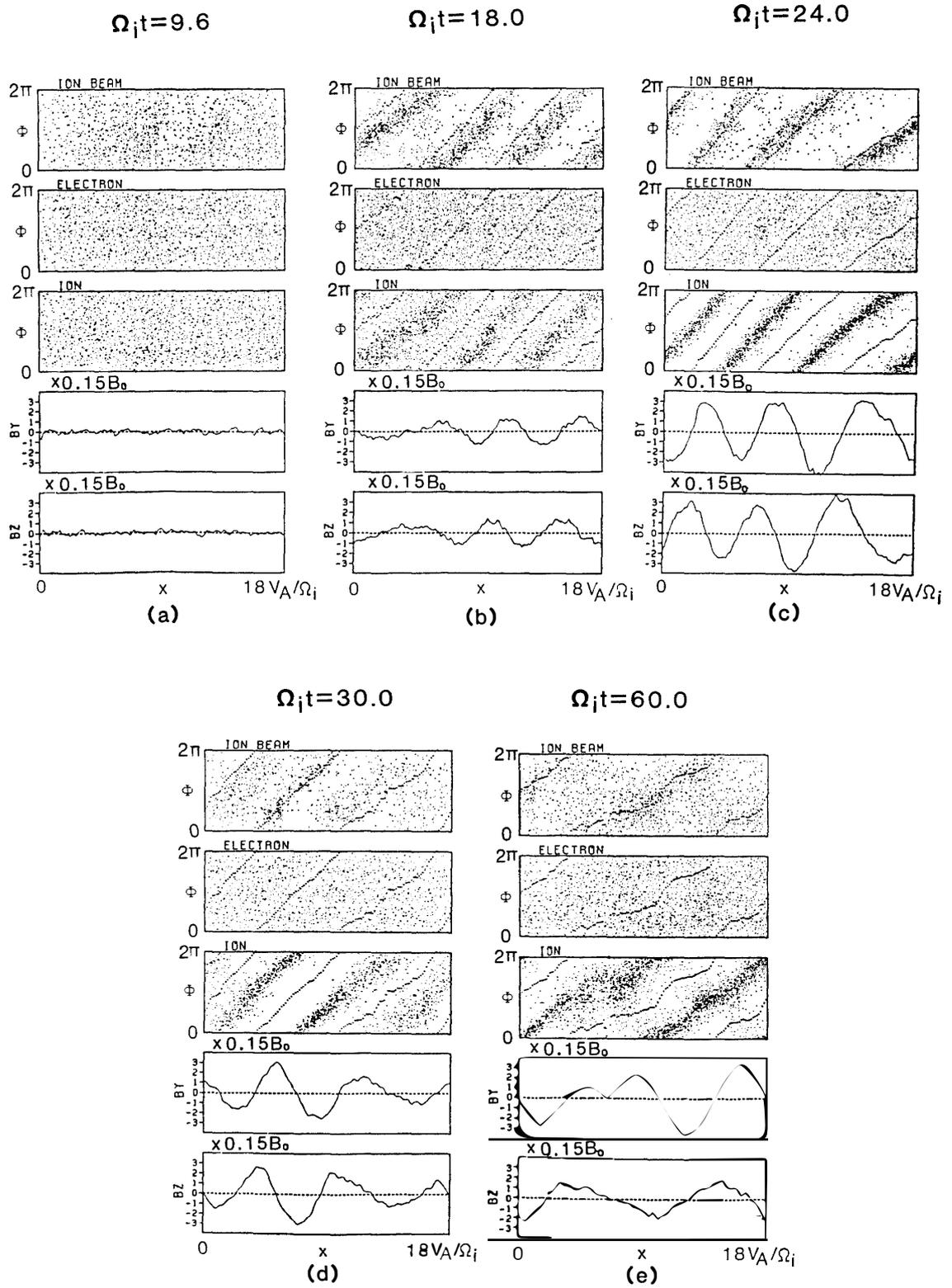
Fig. 6.   Simulation results: $\Phi - x$ plane (upper three panels) and the spatial variation of B_y and B_z (bottom panels) at various times.

the other hand, their phase angles delay by $\sim \pi/2$ behind those of the wave magnetic field in the 'linear' phase (Fig. 6b). This simply means that the perpendicular electric current $j_\perp$ carried by the beam ions is the energy source of the waves ($j_\perp \cdot \delta E < 0$, where δE is the wave electric field). Note that the wave electric field has a phase angle advanced by $\pi/2$ from those of the wave magnetic field, $\delta B = k \times \delta E/\omega$, in terms of the current definition of the phase angle (which makes a left-hand coordinate system).

At $\Omega_i t = 24$, the phase angles of beam ions are slightly advanced from that of the magnetic field, so that $j_\perp \cdot E > 0$. Around this time, we observe an energy transfer from the wave to the beam ions (Fig. 2). As time proceeds further, the phase angle difference becomes nearly zero. This indicates that the beam ions are bunched around Φ_B (see the next section). To the end of this simulation run ($\Omega_i t = 60$, Fig. 6e), this phase bunching effect on the beam ions does not disappear completely but becomes weak. The 'diffuseness' of the beam ion distribution in this phase space plot can be taken as a measure of the pitch angle randomization (scattering) effect. It is noted that in Fig. 6 we see no peculiar behavior of the electrons. This is an evidence that the electrons only play a role of the background medium in this instability process.

We note the angular relation between the bunched beam ions and the waves. We found $\Phi \sim \Phi_B$, namely the perpendicular velocity of the beam ions, $V_\perp$, is parallel to δB. Since the parallel velocity, $V_\parallel$, is a coordinate-dependent variable, it is possible to choose a coordinate system in which the total velocity $V \equiv V_\parallel + V_\perp$ is parallel to the local magnetic field $B \equiv B_0 + \delta B$. The problem is, however, to see the angular relation between V and B in some physically meaningful coordinate system, such as the wave rest frame, or the plasma rest frame.
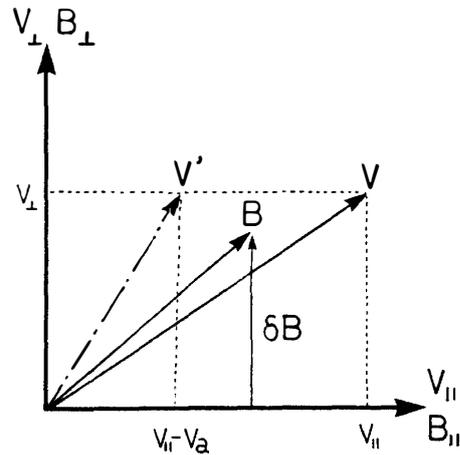

Fig. 7. Relation between magnetic field and beam ion velocity in wave rest frame (*solid line*) and in plasma rest frame (*dashed line*).

In the wave rest frame, the simulation result shows $|V'_\perp|/|V'_\parallel| = 0.55$ and $|\delta B|/B_0 = 0.31$, so that V' is not parallel to B. (" ' " denotes quantities in the wave rest frame. See the illustration in Fig. 7.) On the other hand, in the plasma rest frame (the center-of-mass frame) $|V_\perp|/|V_\parallel|$ is less than $|\delta B|/B_0$ in our simulation. In other words, V is not parallel to B also in the plasma rest frame. (For further discussion, see the next section.)

In Fig. 6, we see a wavelength change in the excited waves (from short to long wavelength): During the 'linear' and early 'nonlinear' phases ($\Omega_i t < 30$, Figs. 6b–6d),

the dominant waves in the system are of the mode 3. In the final stage ($\Omega_i t = 60$, Fig. 6e), the dominant waves become of the mode 2. We interpret this mode conversion to be caused by the nonlinear effect of the excited waves.

We note that this mode conversion is not an artifact caused by the limited system size. In another simulation run, in which the system size is doubled (256 spatial meshes and 9192×3 simulation particles), we found the same nonlinear behavior: Initially the waves of mode 6 and 7 are excited, and eventually these waves are converted to the waves of mode 4. (The waves of mode 6 and 4 correspond to the waves of mode 3 and 2 shown in the above, respectively.)

4. Discussion

The present simulation results show that the system with the parallel ion beam is unstable to the excitation of right-hand polarized electromagnetic waves. This result is consistent with the expectation from the linear stability analysis.

As noted in Section 2, the realistic parameters for the upstream beam ions, such as the beam velocity and the beam density, could not be taken because of the technical/economical reason. To apply our simulation results to the upstream phenomena, therefore, it is necessary to ascertain that the same physical mechanism works in the different parameter regimes. Toward this goal, we also started a three-fluid simulation, in which the three components, the beam ions, the background ions, and the electrons are treated as separate fluids. The basis of this fluid model is two-fold: First, the instability we are treating is of the "fluid type", namely the bulk of the beam ions becomes the source of the free energy. Second, we observed in the full-particle simulation that the individual particle effect, the pitch angle randomization (scattering) effect in the present case, seems to become important only after the middle of the nonlinear phase of the instability (see Fig. 6). We expect, therefore, that the initial phase of the instability could be treated by using the fluid model.

Comparison between the results of the full-particle and the fluid simulations was successful. By using the fluid model, we could reproduce the evolution of the right hand waves and the trapping of the bulk of the beam ions. By the fluid simulation, where a choice of the wide range of parameters is possible, we have confirmed that the governing physical mechanism for the upstream parameters is the same as the one we found in the present full-particle simulation. It is important to note that in the hybrid simulation with more realistic parameters the same phase trapping phenomena are observed (Winske, private communication, 1984).

As these waves grow in amplitude, we observed formation of the crescent-shaped distribution for the beam ions in the phase space (V_x-V_y plane, see Fig. 4). If we compare this crescent-shaped distribution with the observation of the 'intermediate' ions (e.g. Paschmann et al., 1981), we find a close resemblance. It might be thought that this crescent-shaped distribution in the simulation is the manifestation of the randomization of pitch angles. It is not, however, the case for the earlier phase of the instability evolution. As seen in Fig. 6, the beam ions are first bunched in the phase space by the excited waves. The distribution of beam ions at $\Omega_i t = 24$, for example (see Fig. 4b), has a crescent shape because of the projection effect along the spatial

axis (the x-axis). The distribution of the beam ions at every spatial point shows "bunched" behavior, namely beam ions have almost the same velocity $V_\perp$ locally and have not become "diffuse" yet. Only after the bunching is getting weak along with the nonlinear evolution of the waves (at $\Omega_i t > 30$), we observe the nonlinear randomization of the pitch angles, as well as the phase angles.

The above conclusion from the simulation would be worthwhile for further analysis of the observed 'intermediate' ions: Some of these ions would be phase-space bunched ions, whose apparent crescent-shaped distribution in the velocity space is an artifact produced in the data reduction procedure. THOMSEN et al. (1985) arrived at the same conclusion from the detailed analysis of the ion observation. They showed an example in which the ions so far identified as the intermediate ions actually are gyrophase bunched.

We propose here that the phase-bunching process by the excited waves is the origin of the 'gyrophase bunched' ions observed in the upstream region: The 'reflected' ions from the bow shock excite the hydromagnetic waves, which then trap their parent ions as seen in the simulation results. Our proposal here, of course, is not an attempt to exclude the other possibility such as an injection of the gyrophase bunched ions from the specular reflection process at the bow shock. As noted in the introduction, however, these ions are rapidly gyrophase mixed after the injection, so that their existence should be limited to the region adjacent to the shock front. Our mechanism can, on the other hand, explain the 'gyrophase bunched' ions observed in the deeper upstream region.

We analyze here the dynamics of the nonlinear phase bunching of beam ions in large amplitude electromagnetic wave fields. The phase bunching of particles is not a new idea, but has been considered for the case of the electron-whistler interaction (e.g., see the review papers by HELLIWELL, 1974 and MATSUMOTO, 1979), and for the case of the He^+ energization observed in the inner magnetosphere (MAUK, 1982). In a given wave field, the equation of motion for ions can be written in the following form (see the above review papers),

$$\frac{dV_{\parallel}}{dt} = \Omega_w V_\perp \sin \psi , \tag{4}$$

$$\frac{dV_\perp}{dt} = -\Omega_w \left(V_{\parallel} - \frac{\omega}{k} \right) \sin \psi , \tag{5}$$

$$\frac{d\psi}{dt} = -k(V_{\parallel} - V_R) + \frac{\Omega_w}{kV_\perp}(\omega - kV_{\parallel}) \cos \psi , \tag{6}$$

where $\psi \equiv \Phi - \Phi_B$ is the difference between the phase angles of the particle velocity ($V_\perp \equiv V_\perp \sin \Phi e_y + V_\perp \cos \Phi e_z$) and of the wave magnetic field ($\delta B \equiv \delta B \sin \Phi_B e_y + \delta B \cos \Phi_B e_z$) (see Fig. 5). V_R is the resonant velocity defined as $(\omega + \Omega_i)/k$. If the wave satisfy the cyclotron resonance condition eq. (1), V_R becomes identical with the ion beam velocity V_b. Ω_w is defined as $e\delta B/m_i c$ (here the wave amplitude is assumed to be constant). Note that eqs. (4)–(6) are written in the plasma rest frame.

From eqs. (4)–(6), we can show that there is a constant of motion, χ, defined as

$$\frac{1}{2} m_i (V_{\parallel} - V_R)^2 - \frac{m_i \Omega_w V_\perp}{k} \cos \psi \equiv \chi . \tag{7}$$
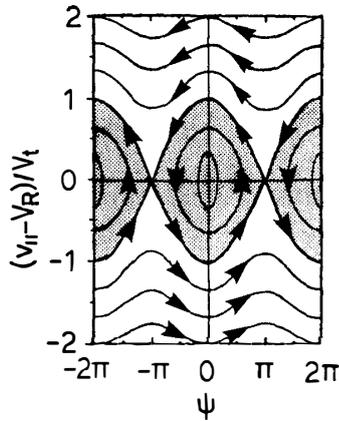
Fig. 8.   *Phase diagram in the $(V-\psi)$ space for trapped and untrapped ions in the wave field. Dotted area shows a phase-trapping region.*

It can be shown that for the resonant ions $(V_{||} \sim V_{R})$ $V_{\perp}$ becomes almost constant. For these particles, we can draw the constant-χ curves in the $V_{||}-\psi$ plane (Fig. 8). The arrows on the curves show the directions of motion in this phase space.   As seen in this figure, there are trapped orbits around the point $V_{||}=V_{R}$ and $\psi=0$.   As drawn in Fig. 8, the trapping orbit is limited for the range, $|V_{||}-V_{R}|<V_{t}\equiv 2(V_{\perp}\Omega_{w}/k)^{1/2}$. If we neglect the terms of the order $B_{\perp}^{2}$, we obtain the pendulum equation for ψ,

$$\frac{d^{2}\psi}{dt^{2}} + \omega_{t}^{2}\sin\psi = 0 , \tag{8}$$

which describes the trapping oscillation around $\psi=0$ (or $\Phi=\Phi_{B}$) with the trapping frequency ω_{t} defined as $(kV_{\perp}\Omega_{w})^{1/2}$.

The above simple analysis explains the phase bunching of beam ions observed in the simulation.   From eq. (6), we can get further information about the angular relation between the velocity $(V\equiv V_{||}+V_{\perp})$ of the bunched beam ions and the local magnetic field $(B\equiv B_{0}+\delta B)$.   Assuming $\psi=0$, we obtain,

$$\frac{V'_{\perp}}{V'_{||}} \equiv \frac{V_{\perp}}{V_{||}-V_{a}} = \frac{kV_{\perp}+\Omega_{w}}{\Omega_{i}} , \tag{9}$$

where we assumed $\omega/k=V_{a}$. $V'_{\perp}$ and $V'_{||}$ are the velocity components in the wave rest frame.   Using the relation of $\omega_{t}^{2}=kV_{\perp}\Omega_{w}$, we get,

$$\frac{V'_{\perp}}{V'_{||}} = \frac{\Omega_{w}}{\Omega_{i}}\left(1+\frac{\omega_{t}^{2}}{\Omega_{w}^{2}}\right) > \frac{\Omega_{w}}{\Omega_{i}} = \frac{B_{\perp}}{B_{0}} . \tag{10}$$

This shows that the bunched ion velocity is not parallel to the local magnetic field in the wave rest frame (Fig. 7).   To see the angular relation between V and B in the plasma rest frame, the knowledge of the amplitudes of $V_{\perp}$ and δB is necessary.   The simulation result shows that $V_{\perp}/V_{||}$ is smaller than $\delta B/B_{0}$ (see the previous section.)   However, the three-fluid simulation with more realistic parameters gives us the result of $V_{\perp}/V_{||}>\delta B/B_{0}$.   We generally found that V is not parallel to B in both the plasma and wave rest frames.

It is interesting to note that in THOMSEN *et al.*'s observations (see their Fig. 1) the "gyrophase bunched" ions have $V_{\perp}$ (the perpendicular component with respect

to the average magnetic field), which is in the same direction as the wave magnetic field δB. This is consistent with the expectation based on the phase-bunching mechanism. The observed total velocity of the beam $V \equiv V_{\parallel} + V_{\perp}$ in the solar wind frame is to be not parallel to the local magnetic field, $B \equiv B_0 + \delta B$, which is again consistent with our simulation result.

In the nonlinear phase of the excited waves in the simulation, the phase bunching of beam ions becomes ambiguous as the energy transfer among the several wave modes occurs. In our simulation, this energy transfer occurs from short to long wavelength, which would be caused by the decay (or modulational) instability. The decay instability process for large amplitude electromagnetic waves has been considered by LASHMORE-DAVIES (1976), GOLDSTEIN (1978), and SAKAI and SONNERUP (1983). In a separate simulational work, WINSKE and LEROY (1984) have also observed the wave decay phenomena. In their case, however, the wave energy is transformed from long to short wavelength, which is the opposite energy-flow direction from ours. Further, their decay process takes place quite rapidly. The mode transformation occurs within one trapping period right after the linear wave growing phase ends. In our simulation, on the contrary, the mode transformation occurs slowly, taking the time of a few trapping periods ($\sim 30 \; \Omega_i^{-1}$). The above differences may be due to the difference in the amplitude of the excited waves. The wave amplitude ($\sim 100\%$ of the ambient field) in their simulation is larger than ours ($\sim 50\%$). Recently, WINSKE (1984, private communication) made simulations with parameters similar to ours, where the wave amplitude is $\sim 40\%$ and the decay behavior of the excited waves is found to be weaker. On these wave decay behaviors, we are now making further studies by extending the parameter choices in the simulation, the result of which will appear as the second part of the series of papers.

Acknowledgments

References

ASBRIDGE, J. R., BAME, S. J. and STRONG, I. B. (1968): Outward flow of protons from the earth's bow shock. J. Geophys. Res., 73, 5777–5782.

BARNES, A. (1970): Theory of generation of bow-shock-associated hydromagnetic waves in the upstream interplanetary medium. Cosmic Electrodyn., 1, 90–114.

BONIFAZI, C. and MORENO, G. (1981a): Reflected and diffuse ions backstreaming from the earth's bow shock, 1. Basic properties. J. Geophys. Res., 86, 4397–4404.

BONIFAZI, C. and MORENO, G. (1981b): Reflected and diffuse ions backstreaming from the earth's bow shock, 2. Origin. J. Geophys. Res., 86, 4405–4413.

BONIFAZI, C., EGIDI, A., MORENO, G. and ORSINI, S. (1980): Backstreaming ions outside the earth's bow shock and their interaction with the solar wind. J. Geophys. Res., 85, 3461–3472.

EASTMAN, T. E., ANDERSON, R. R., FRANK, L. A. and PARKS, G. K. (1981): Upstream particles observed in the earth's foreshock region. J. Geophys. Res., 86, 4379–4395.

FAIRFIELD, D. H. (1969): Bow shock associated wave observed in the far upstream interplanetary medium. J. Geophys. Res., 74, 3541–3553.

Gary, S. P. (1981): Microinstabilities upstream of the earth's bow shock; A brief review. J. Geophys. Res., **86**, 4331–4336.

Gary, S. P., Gosling, J. T. and Forslund, D. W. (1981): The electromagnetic ion beam instability upstream of the earth's bow shock. J. Geophys. Res., **86**, 6691–6696.

Goldstein, M.L. (1978): An instability of finite amplitude circularly polarized Alfvén waves. Astrophys. J., **219**, 700–704.

Gosling, J. T., Asbridge, J. R., Bame, S. J., Paschmann, G. and Sckopke, N. (1978): Observations of two distinct populations of bow shock ions. Geophys. Res. Lett., **5**, 957–960.

Gosling, J. T., Thomsen, M. F., Bame, S. J., Feldman, W. C., Paschmann, G. and Sckopke, N. (1982): Evidence for specularly reflected ions upstream from the quasi-parallel bow shock. Geophys. Res. Lett., **9**, 1333–1336.

Greenstadt, E. W., Russell, C. T. and Hoppe, M. M. (1980): Magnetic field orientation and suprathermal ion streams in the earth's foreshock. J. Geophys. Res., **85**, 3473–3479.

Greenstadt, E. W., Hoppe, M. M. and Russell, C. T. (1982): Large-amplitude magnetic variations in quasi-parallel shocks; Correlation lengths measured by ISEE 1 and 2. Geophys. Res. Lett., **9**, 781–784.

Gurgiolo, C., Parks, G. K., Mauk, B. H., Lin, C. S., Anderson, K. A., Lin, R. P. and Reme, H. (1981): Non-$E \times B$ ordered ion beams upstream of the earth's bow shock. J. Geophys. Res., **86**, 4415–4424.

Gurgiolo, C., Parks, G. K. and Mauk, B. H. (1983): Upstream gyrophase bunched ions; A mechanism for creation at the bow shock and the growth of velocity space structure through gyrophase mixing. J. Geophys. Res., **88**, 9093–9100.

Helliwell, R. A. (1974): Controlled VLF wave injection experiments in the magnetosphere. Space Sci. Rev., **15**, 781–802.

Hoppe, M. M. and Russell, C. T. (1983): Plasma rest frame frequencies and polarizations of the low-frequency upstream waves; ISEE 1 and 2 observations. J. Geophys. Res., **88**, 2021–2028.

Hoppe, M. M., Russell, C. T., Frank, L. A., Eastman, T. E. and Greenstadt, E. W. (1981): Upstream hydromagnetic waves and their association with backstreaming ion populations; ISEE 1 and 2 observations. J. Geophys. Res., **86**, 4471–4492.

Hoppe, M. M., Russell, C. T., Eastman, T. E. and Frank, L. A. (1982): Characteristics of the ULF waves associated with upstream ion beams. J. Geophys. Res., **87**, 643–650.

Lashmore-Davies, C. N. (1976): Modulational instability of a finite amplitude Alfvén wave. Phys. Fluids, **19**, 587–589.

Lemons, D. S., Asbridge, J. R., Bame, S. J., Feldman, W. C., Gary, S. P. and Gosling, J. T. (1979): The source of electrostatic fluctuations in the solar wind. J. Geophys. Res., **84**, 2135–2138.

Mauk, B. H. (1982): Electromagnetic wave energization of heavy ions by the electric "phase bunching" process. Geophys. Res. Lett., **9**, 1163–1166.

Matsumoto, H. (1979): Nonlinear whistler-mode interaction and triggered emission in the magnetosphere; A review. Wave Instabilities in Space Plasmas, ed. by P. J. Palmadesso and K. Papadopoulos. Dordrecht, D. Reidel, 163–190.

Palmadesso, P. and Schmidt, G. (1971): Collisionless damping of a large amplitude whistler wave. Phys. Fluids, **14**, 1411–1418.

Paschmann, G., Sckopke, N., Bame, S. J., Asbridge, J. R., Gosling, J. T., Russell, C. T. and Greenstadt, E. W. (1979): Association of low-frequency waves with suprathermal ions in the upstream solar wind. Geophys. Res. Lett., **6**, 209–212.

Paschmann, G., Sckople, N. and Papamastorakis, I. (1981): Characteristics of reflected and diffuse ions upstream from the earth's bow shock. J. Geophys. Res., **86**, 4355–4364.

Sakai, J.-I. and Sonnerup, B. U. O. (1983): Modulational instability of finite amplitude dispersive Alfvén waves. J. Geophys. Res., **88**, 9069–9079.

Scarf, F. L., Fredricks, R. W., Frank, L. A., Russell, C. T., Coleman, P. J., Jr. and Neugebauer, M. (1970): Direct correlations of large-amplitude waves with superthermal protons in the upstream solar wind. J. Geophys. Res., **75**, 7316–7322.

SENTMAN, D. D., EDMISTON, J. P. and FRANK, L. A. (1981): Instabilities of low frequency, parallel propagating electromagnetic waves in the earth's foreshock region. J. Geophys. Res., **86**, 7487–7497.

SENTMAN, D. D., THOMSEN, M. F., GARY, S. P., FELDMAN, W. C. and HOPPE, M. M. (1983): The oblique whistler instability in the earth's foreshock. J. Geophys. Res., **88**, 2048–2056.

THOMSEN, M. F., GOSLING, J. T., BAME, S. J. and RUSSELL, C. T. (1985): Gyrating ions and large-amplitude monochromatic MHD waves upstream of the earth's bow shock. J. Geophys. Res., **90**, 267–273.

WATANABE, Y. and TERASAWA, T. (1984): On the excitation mechanism of upstream low frequency waves. J. Geophys. Res., **89**, 6623–6630.

WINSKE, D. and LEROY, M. M. (1984): Diffuse ions produced by electromagnetic ion beam instabilities. J. Geophys. Res., **89**, 2673–2688.